

# A HIGH-PERFORMANCE PLL OBSERVER FOR SENSORLESS THREE-PHASE INDUCTION MOTOR CONTROL

Emerson G. Carati<sup>1</sup>, Felipe S. D. Sant<sup>1</sup>, Diego D. Pinheiro<sup>1</sup>

<sup>1</sup>Universidade Tecnológica do Paraná (UTFPR), Campus Pato Branco – Paraná, Brazil  
e-mail: emerson@utfpr.edu.br, diego.npn@gmail.com

**Abstract** – This paper presents an enhanced estimation algorithm based on the PLL (phase-locked loop) approach, which is used to estimate the rotor speed in induction motors (IM) drives. It can be challenging to obtain an accurate estimate during frequency ramps using existing PLL schemes. Thus, the performance of PLL schemes can be degraded during the acceleration and deceleration operations when applied to motor drives. In addition, the performance of conventional PLL scheme estimation is negatively affected by disturbances, for example, DC offsets. One of the novelties of the proposed speed observer (HPPO - High-Performance PLL Observer) is error normalization, which is based on the currents and a mechanism of variable gain based on the reference speed. The reference speed is also used to build an additional feedforward adjustment action. These modifications improve estimator results during load insertions and at low rates. In order to validate the proposed HPPO algorithm, it is implemented experimentally in a laboratory prototype using a 2.2kW IM. The motor is driven by a three-phase pulse width modulation (PWM) power converter, which is controlled by a DSP TMS320F28069. Numerical analysis and experimental results are carried out to validate the proposed scheme's high performance.

**Keywords** – Field Oriented Control, Induction Machine, Phase Locked Loop, Speed Control, Speed Sensorless.

## NOMENCLATURE

$\vec{v}_s$	$\Re^{(2 \times 1)}$ Stator voltages vector.
$\vec{i}_s, \vec{i}_r$	$\Re^{(2 \times 1)}$ Stator and rotor currents vector.
$\vec{\psi}_s, \vec{\psi}_r$	$\Re^{(2 \times 1)}$ Stator and rotor fluxes vector.
$R_s, R_r$	Stator and rotor resistances.
$L_s, L_r$	Stator and rotor inductances.
$L_m$	Magnetizing inductance.
$p$	Pole pair number.
$\omega$	Angular generic speed of the reference frame.
$\omega_r$	Angular rotor speed.
$\hat{\omega}_r$	Estimated angular rotor speed.
$\omega_r^*$	Reference rotor speed.
$\omega_{nom}$	Rated rotor speed.
$T, T_L$	Electromagnetic torque and load torque.
$J, D$	Rotor inertia and viscous friction coefficient.
$\Psi_{dr}, \Psi_{qr}$	Rotor fluxes in $dq$ -axes.
$i_{ds}, i_{qs}$	Stator currents in $dq$ -axes.
$i_{dr}, i_{qr}$	Rotor currents in $dq$ -axes.

$i_{\alpha s}, i_{\beta s}$	Stator currents in $\alpha\beta$ -axes.
$i_{\alpha sf}, i_{\beta sf}$	Stator currents filtered in $\alpha\beta$ -axes.
$i_{as}, i_{bs}, i_{cs}$	Three-phase stator currents.
$\tau_{is}$	Current loop time constant.
$\beta_{is}$	Current loop plant gain.
$\tau_{\omega r}$	Speed loop time constant.
$\beta_{\omega r}$	Speed loop plant gain.
$\tau_{ri} = \frac{R_r}{L_r}$	Inverse rotor time constant.
$\xi$	Ratio damping.
$\omega_n$	Natural frequency.
$t_s$	Settling time.
$K_p$	Proportional gain.
$K_i$	Integral gain.
$K_{FF}$	Reference speed gain.
$\varepsilon$	Error angle signal.
$\bar{\varepsilon}$	Normalization of the error angle signal.
$f_c$	Frequency of the low-pass filter.
$f_s$	Switching frequency.
$T_s$	Sampling time.
$\hat{\phantom{x}}$	Symbol indicates estimation.
*	Symbol indicates reference/command.

## I. INTRODUCTION

The induction motor (IM) is widely used in the industry for its well-known advantages, such as simple construction, less maintenance, reliability, and low cost. The IM is considered a multiple-input and multiple-output (MIMO) system. It requires complicated differential equations to describe its mathematical behavior [1], [2]. The electromechanical variables of the motor must be properly controlled to meet technological demands in different applications. One of the industry-standard control techniques for IM has been field-oriented control (FOC), established firstly in [3] with a cascade structure. Because of the coupling between state variables, FOC requires a complex structure using proportional-integral (PI) controllers as a traditional approach to vector control [4]. In the last decades, different control structures have been used to replace PI controllers in the vector control approach, such as fuzzy logic [5], [6], artificial neural network (ANN) [7], [8], sliding mode [9]–[12], super-twisting sliding mode [13]–[15].

The main techniques used in FOC are direct field orientation control (DFOC) and indirect field orientation control (IFOC). The DFOC technique requires additional estimators or hall effect sensors to obtain the rotor flux position directly. The IFOC technique obtains the rotor flux position through indirect estimation [16] using the estimated speed/position. These approaches provide torque or speed control of the induction motor by decoupling the torque and flux. There are different ways of implementing the vector

control strategy according to the choice of reference frames for the space vectors. The main flux space vectors in induction motors are air gap flux, stator flux, and rotor flux.

The IFOC technique is based on the IM model, and its operation is highly dependent on the parameters of the machine, such as resistances and inductances. In [17], the IM model is described in detail, which depends on the machine parameters, which are variable because of temperature, saturation levels, and frequency, among others. In general, the parameter mismatch and the noise in the input signals of the flux model cause the conventional speed estimation techniques to fail at very low-speed operation in sensorless high-performance IM drives.

In IM, the position of the rotor flux vector is dependent on the rotational speed of the machine. Moreover, the knowledge of the rotor speed is also necessary for the speed control performed by the vector drive system, which requires feedback on the mechanical speed of the motor for comparison with the reference speed. The rotor speed can be measured through a sensor or may be estimated using voltages, current signals, and machine parameters. The use of a mechanical speed sensor simplifies the implementation of the IFOC system. However, it makes the project more expensive due to the cost of the speed sensor and the other circuits for conditioning and instrumentation [18]. Physical speed sensors are associated with problems, such as mechanical robustness reduction of the drive, shaft extension, and cost increase. To overcome these problems, several speed estimators for sensorless vector control of IM have been developed, such as open-loop estimators using improved schemes [17], [19], [20], model reference adaptive systems (MRAS) [21]–[23], adaptive observers [24], estimators using ANN [25], in particular, neural networks and fuzzy logic systems, sliding mode observers [26]–[28] and phase locked loop (PLL) [29]–[34]. Generally, the drive performance of sensorless control methods is excellent, depending on speed range and if the machine is accurately identified and the algorithm is calibrated accordingly. However, the high efforts for implementation and calibration and the corresponding computational burden are major reasons for the limited practical application of these methods.

The speed sensorless control presented in this paper is characterized as an enhanced PLL algorithm. It uses the main characteristics of the traditional PLL as seen in [32], [33], [35] and improves with error normalization based on the currents and a mechanism of variable gain based on reference speed. Additionally, the reference speed is also used to build an auxiliary feedforward adjustment action. These modifications improve estimator results during load insertions and at low and zero speeds. This paper is organized as follows: Section II presents the three-phase induction motor model, while in Section III, the vector control strategy is shown, using the indirect field-oriented control with rotor flux alignment. Section IV presents the structure of the traditional PLL and the proposed High-Performance PLL Observer (HPPO). Section V accomplishes the numerical analysis of sensorless closed-loop drive using Matlab® environment. The experimental evaluation with a PWM inverter-driven IM is carried out and discussed in Section VI. The key features of the HPPO are

discussed in Section VII.

## II. THREE-PHASE INDUCTION MOTOR MODEL

For the modeling of the induction machine, the following assumptions were made:

- Only the fundamental wave of the air-gap field is considered for the calculation of the inductances;
- The neutral point is not connected;
- There are no eddy currents or core losses in the stator and rotor.

Using these assumptions, which are common to the modeling of electrical machines, the induction machine will be described by the following well-known set of complex equations (1) and (2) in the generic reference frame [36]:

$$\vec{v}_s = \vec{i}_s R_s + j\omega \vec{\psi}_s + \frac{d}{dt} \vec{\psi}_s, \quad (1)$$

$$0 = \vec{i}_r R_r + j(\omega - p\omega_r) \vec{\psi}_r + \frac{d}{dt} \vec{\psi}_r. \quad (2)$$

The fluxes and currents are related by (3) and (4)

$$\vec{\psi}_s = L_s \vec{i}_s + L_m \vec{i}_r, \quad (3)$$

$$\vec{\psi}_r = L_m \vec{i}_s + L_r \vec{i}_r. \quad (4)$$

The motion equation is shown in (5)

$$T - T_L = J \frac{d\omega_r}{dt} + D\omega_r, \quad (5)$$

and the electromagnetic equation is related by (6)

$$T = \frac{3}{2} p \frac{L_m}{L_r} (\vec{\psi}_r \times \vec{i}_s). \quad (6)$$

## III. Vector Control Strategy

The objective of field-oriented control or vector control with rotor flux alignment is the decoupling between magnetic flux and torque of the machine to obtain a good performance IM drives. Then,

$$\psi_{dr} = |\psi_r|, \quad (7)$$

$$\psi_{qr} = 0. \quad (8)$$

Assuming that the rotor flux vector is aligned to the direct, and with that, replacing (7) and (8) in (3) and (4), it results:

$$i_{dr} = -\frac{L_m}{L_r} i_{ds} + \frac{|\psi_r|}{L_r}, \quad (9)$$

$$i_{qr} = -\frac{L_m}{L_r} i_{qs}. \quad (10)$$

Rearranging (9) and (10) in (2), the following equations (11) and (12) are obtained,

$$|\psi_r|(\omega - p\omega_r) - i_{qs} \frac{R_r L_m}{L_r} = 0, \quad (11)$$

$$\frac{d}{dt} |\psi_r| + |\psi_r| \frac{R_r}{L_r} - i_{ds} \frac{R_r L_m}{L_r} = 0. \quad (12)$$

Moreover, from (6), the electromagnetic torque is obtained on the  $dq$ -axes in (13):

$$T = \frac{3}{2} p \frac{L_m}{L_r} (\Psi_{dr} i_{qs} - \Psi_{qr} i_{ds}). \quad (13)$$

In steady state from equations (11) and (12), it can be obtained:

$$|\Psi_r| = L_m i_{ds}, \quad (14)$$

$$\omega = p \omega_r + \frac{R_r}{L_r} \frac{i_{qs}}{i_{ds}}. \quad (15)$$

Using (13), (14) and (15), a new expression for the electromagnetic torque can be obtained in (16),

$$T = \frac{3}{2} p \frac{L_m^2}{L_r} i_{ds} i_{qs}. \quad (16)$$

The decoupling of the rotor flux and electromagnetic torque variables of the FOC structure with alignment on the  $d$ -axis, can be seen in equations (14) and (16).

Figure 1 shows the control structure used to perform current and voltage machine driving for a given speed reference and flux reference. In Figure 1  $\omega_r^*$  is the reference rotor speed,  $\Psi_r^*$  is the rotor flux reference,  $i_{ds}^*$  and  $i_{qs}^*$  are the reference stator currents. The FOC approach uses PI controllers to generate output voltages  $v_{ds}$  and  $v_{qs}$ , which are used to drive the motor using pulse width modulation (PWM) modulation.

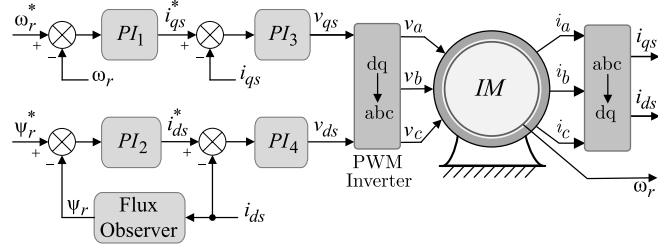


Fig. 1. Topology of the IFOC vector control system.

The gains of the four PI controllers were calculated according to the well-known method presented in [35]:

$$K_{P1} = \frac{8\tau_{\omega_r} - t_s}{t_s \beta_{\omega_r}}, \quad (17) \quad K_{I1} = \frac{16\tau_{\omega_r}}{t_s^2 \xi^2 \beta_{\omega_r}}, \quad (20)$$

$$K_{P2,4} = \frac{8\tau_{i_s} - t_s}{t_s \beta_{i_s}}, \quad (18) \quad K_{I2,4} = \frac{16\tau_{i_s}}{t_s^2 \xi^2 \beta_{i_s}}, \quad (21)$$

$$K_{P3} = \frac{8}{t_s L_m} - t_s, \quad (19) \quad K_{I3} = \frac{16}{t_s^2 \xi^2 L_m}. \quad (22)$$

#### IV. THE PLL SENSORLESS APPROACH

The Phase-Locked Loop (PLL) algorithms emerged in electrical power engineering as grid voltage zero crossing detection for grid commutated or active rectifiers. It is well known that the pursuit of the accurate determination of frequency and angle constitutes a trade-off. Recently, the PLL concept also has been used to estimate the mechanical rotor speed of the IM [34]. The basic algorithm is based on a conventional quadrature PLL.

##### A. Conventional PLL Observer (CPLL)

Conventional PLL (CPLL) can be applied to estimate the rotor speed using the stator currents in the stationary frame of reference through the Clarke transformation. The mathematical model also considers the Park transformation for angle synchronization. This section introduces the PLL concept and its algorithm for rotor speed estimation, as shown in Figure 2.

Assuming a set of balanced three-phase electric currents, the current vector  $\vec{i}_s$  can be written as

$$\vec{i}_s = \begin{bmatrix} i_{as} \\ i_{bs} \\ i_{cs} \end{bmatrix} = I_s \begin{bmatrix} \sin(\theta) \\ \sin(\theta - \frac{2\pi}{3}) \\ \sin(\theta + \frac{2\pi}{3}) \end{bmatrix}. \quad (23)$$

The Clarke transformation may be used to obtain currents in direct ( $0^\circ$ ) and quadrature ( $+90^\circ$ ) coordinates as

$$\begin{bmatrix} i_{\alpha s} \\ i_{\beta s} \end{bmatrix} = \frac{2}{3} \begin{bmatrix} 1 & -\frac{1}{2} & -\frac{1}{2} \\ 0 & \frac{\sqrt{3}}{2} & -\frac{\sqrt{3}}{2} \end{bmatrix} \begin{bmatrix} i_{as} \\ i_{bs} \\ i_{cs} \end{bmatrix}. \quad (24)$$

Considering that currents are assumed to be sinusoidal and balanced, (24) can be rewritten as follows:

$$\begin{bmatrix} i_{\alpha s} \\ i_{\beta s} \end{bmatrix} = \begin{bmatrix} i_{as} \\ \frac{\sqrt{3}}{3}(i_{bs} - i_{cs}) \end{bmatrix}. \quad (25)$$

The Park transform can be used to obtain the direct and quadrature currents in synchronous reference, as

$$\begin{bmatrix} i_{ds} \\ i_{qs} \end{bmatrix} = \begin{bmatrix} \cos(\hat{\theta}) & \sin(\hat{\theta}) \\ -\sin(\hat{\theta}) & \cos(\hat{\theta}) \end{bmatrix} \begin{bmatrix} i_{\alpha s} \\ i_{\beta s} \end{bmatrix}. \quad (26)$$

It can be seen that the transform is performed at the estimated angle ( $\hat{\theta}$ ). Finally, replacing the equation (25) in (26), the following result is obtained in (27):

$$\begin{bmatrix} i_{ds} \\ i_{qs} \end{bmatrix} = \begin{bmatrix} i_{as} & \frac{\sqrt{3}}{3}(i_{bs} - i_{cs}) \\ -\frac{\sqrt{3}}{3}(i_{bs} - i_{cs}) & i_{as} \end{bmatrix} \begin{bmatrix} \cos(\hat{\theta}) \\ \sin(\hat{\theta}) \end{bmatrix}. \quad (27)$$

Since  $\sin(a \pm b) = \sin(a)\cos(b) \pm \sin(b)\cos(a)$ , from (27) it results in (28):

$$\begin{bmatrix} i_{ds} \\ i_{qs} \end{bmatrix} = \begin{bmatrix} I_s \sin(\theta - \hat{\theta}) \\ I_s \cos(\theta - \hat{\theta}) \end{bmatrix}. \quad (28)$$

In (28), it can be seen that when the estimated angle  $\hat{\theta}$  converges to the real angle  $\theta$ , the signal  $i_d$  becomes null. Therefore it can be used as the error signal for the PLL

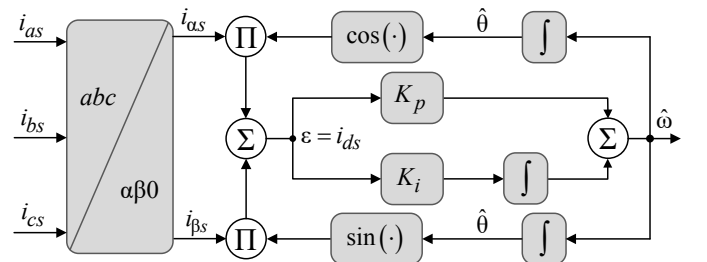


Fig. 2. Block diagram of the conventional PLL observer (CPLL).

observer. Furthermore, the equation for  $i_{ds}$  can be rewritten using linearization. Then, the error is given by (29)

$$\varepsilon = I_s(\theta - \hat{\theta}). \quad (29)$$

In order to obtain error asymptotic convergence to zero, the conventional PLL observer usually utilizes a PI (proportional-integral) adaptation mechanism. From the PLL observer output  $\hat{\omega}$ , the rotor speed can be estimated using the slip expression for the induction motor operating with FOC. So, the estimated rotor speed is given by (30)

$$\hat{\omega}_r = \frac{1}{p} \left( \hat{\omega} - \frac{R_r}{L_r} \frac{i_{qs}}{i_{ds}} \right). \quad (30)$$

Considering the settling time defined as  $t_s = 4.6\tau$ , with  $\tau = \frac{1}{\xi\omega_n}$ , the PLL observer PI controller gains are calculated according to [37], where is shown in (31):

$$K_p = 2\xi\omega_n = \frac{9.2}{t_s}, \quad K_i = \frac{4.6\omega_n}{t_s\xi}, \quad (31)$$

The definition of the settling time  $t_s$  is proposed in [38], which is measured from the start time to the time in which the system stays within 1% of the steady-state response of a particular second-order system responding to a step input.

### B. The Proposed High-Performance PLL Observer (HPPO)

One of the main problems of the PLL technique occurs when the load is connected to the machine shaft. Load insertions cause sudden increases in the electrical currents of the motor. As a result, due to electrical currents being used to obtain the error signal  $\varepsilon$ , the rotor speed estimation is affected, reducing the performance of the PLL observer. Also, in critical cases, this problem can lead the sensorless drive system to instability. Another important observation regarding the rotor speed estimation for electric machine drives is related to the low and/or zero speed ranges, where most approaches have difficulty maintaining high performance and accuracy in the estimation. Thus, the CPLL is modified in order to solve these problems and increase the performance of rotor speed estimation through the PLL technique. The proposed PLL technique is shown in Figure 3, where several improvements are included from the original CPLL structure.

The proposed scheme is named here as *High-Performance PLL Observer (HPPO)* since the included modifications significantly improve the rotor speed estimation. These

modifications include currents filtering, error normalization, gain self-adjustment and reference feedforward. The following subsections describe these techniques in details.

1) *Filter for stator currents:* In practical applications, the stator currents include measurement noise and are usually distorted by high order harmonics, electromagnetic interference (EMI) environment, and other disturbance sources. These distortions also affect the PLL observer. In this work, the currents are smoothed through first-order low-pass filters to reduce the effect of disturbances. The filter output is obtained as shown in (32),

$$i_{\alpha sf} = \frac{2\pi f_c}{s + 2\pi f_c} i_{\alpha s}, \quad i_{\beta sf} = \frac{2\pi f_c}{s + 2\pi f_c} i_{\beta s}. \quad (32)$$

2) *Normalization of the error angle signal:* PLL observer is impacted by sudden changes in stator currents due to load variation. Error signal normalization  $\bar{\varepsilon}$  can be used to overcome the mentioned problem. This mathematical feature guarantees small oscillations during insertion and load removal on the machine shaft. In the HPPO scheme, the signal  $\bar{\varepsilon}$  that is used as the excitation by adjustment mechanism is obtained as shown in (33),

$$\bar{\varepsilon} = \frac{1}{\sqrt{i_{\alpha sf}^2 + i_{\beta sf}^2}} \varepsilon. \quad (33)$$

3) *Self-adjusting speed gain mechanism:* The Normalization of the error signal reduces the oscillations that occur when the load changes on the machine shaft, but it deteriorates the PLL performance at low speeds. In this case, the low frequency of the currents and the modification of the Normalization generate a low excitation input to the PI tuning mechanism. Thereby, the PI controller output convergence time increases significantly, causing a more significant estimation error during this period. Thus, to solve this problem, the PLL structure is modified considering the reference rotor speed  $\omega_r^*$ . This feature introduces two elements based on feedforward, so it is possible to obtain better signals in the estimation, especially at low speeds. The first is a variable gain system, which works only at low speeds. This system modifies the value of the proportional gain of the PI controller, being inversely proportional to the reference speed ( $K_p \propto 1/\omega_r^*$ ), causing it to assume a greater value  $K_0$  at zero reference rotor speed and gradually decreases until

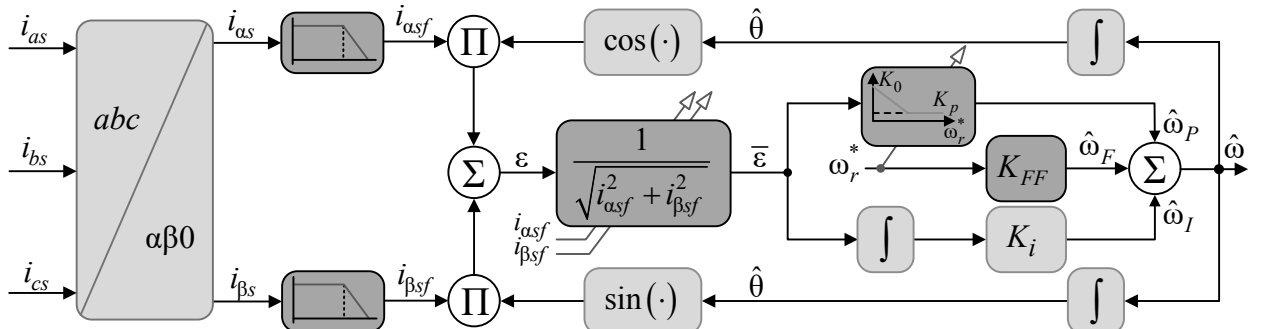


Fig. 3. Block diagram of the High Performance PLL observer (HPPO).

the nominal proportional gain  $K_p$  at  $\gamma\omega_{nom}$  with  $0 < \gamma \ll 1$ . Therefore, the proportional output of the PI controller is obtained through the tuning mechanism as follows in (34):

$$\hat{\omega}_p = \begin{cases} \left( K_0 - \frac{K_0 - K_p}{\gamma\omega_{nom}} \omega_r^* \right) \bar{\epsilon} & \text{if } 0 < \omega_r^* < \gamma\omega_{nom} \\ K_p \bar{\epsilon} & \text{if } \omega_r^* \geq \gamma\omega_{nom} \end{cases}. \quad (34)$$

In addition, the second improvement to the self-adjusting gain mechanism consists of a feedforward action ( $\hat{\omega}_F$ ), which is added to the proportional ( $\hat{\omega}_p$ ) and integral ( $\hat{\omega}_I$ ) components in the speed estimation. The feedforward action applies the ( $K_{FF}$ ) gain to the reference speed, such as is shown in (35)

$$\hat{\omega}_F = K_{FF} \omega_r^*. \quad (35)$$

The feedforward gain is given by  $K_{FF} = p\kappa$ , where  $p$  is the number of poles of the IM and  $0 < \kappa \ll 1$  is a design parameter.

## V. NUMERICAL ANALYSIS

The numerical evaluation was carried out in the Matlab® environment. The motor drive using IFOC vector control and the sensorless techniques was digitally implemented at a 6 kHz sampling frequency. In the simulations, a discrete-time model of the IM is used, which is obtained using the first-order Euler discretization method. The induction motor and load parameters are appropriately defined in simulations for performance comparisons of the emulated system with the experimental one. The IM parameters used in tests are shown in Table I.

**TABLE I**  
**The Three-Phase Induction Motor Parameters**

Parameter	Value	Unit
Rated power ( $P_n$ )	3	HP
Rated voltage ( $V_n$ )	220	V
Rated current ( $I_n$ )	11,1	A
Rated speed ( $\omega_n$ )	1715	rpm
Stator inductance ( $L_s$ )	171	mH
Rotor inductance ( $L_r$ )	171	mH
Mutual inductance ( $L_M$ )	163	mH
Stator resistance ( $R_s$ )	1,72	$\Omega$
Rotor resistance ( $R_r$ )	1,24	$\Omega$
Moment of inertia ( $J$ )	0,0150	$Kgm^2$
Viscous coefficient ( $B_n$ )	0,02	$Nms$

The numerical evaluation of the CPPL and HPPO sensorless techniques for estimating the rotor speed is presented in Figures 4-6, where the rotor speed reference is set to have an acceleration ramp of 225 rpm/s into 2s, where the IM rotor speed reaches a speed of 450 rpm. The rotor flux reference is set to its rated value (0.7 Wb). In addition, a load of 4,175 Nm is connected to the motor shaft at instant 5s.

The upper graph in Figure 4 shows the reference rotor speed, the actual rotor speed, and the CPLL speed estimation. The lower graph in Figure 4 shows the same waveforms for the HPPO technique. Both techniques present good steady-state speed estimation. On the other side, it is possible to verify oscillations on the actual speed at the exact moment of load insertion. However, the oscillation is considerably smaller in

the HPPO technique.

Figure 5 shows the error signals referring to the two sensorless techniques for a better comparison. For the CPLL, it is possible to verify the high error when inserting the load on the machine shaft, reaching peaks greater than 25% ( $e_{max}^{CPLL} > 25\%$ ). For HPPO, the error does not exceed 20%, confirming its better performance ( $e_{max}^{HPPO} < 20\%$ ). The CPLL also presents a relatively lower performance on motor acceleration than the HPPO.

The motor speed reversal test is presented in Figure 6, where the profile of the rotor speed reference is 0 rpm  $\rightarrow$  +450 rpm  $\rightarrow$  -450 rpm. The upper graph waveforms show the performance of the HPPO estimator in the closed-loop. Also is important to observe the proper functioning of the drive system throughout the entire speed range, including the 0 rpm crossing. In the lower graph of Figure 6, it is possible to verify the effect of motor speed reversal in the stator currents.

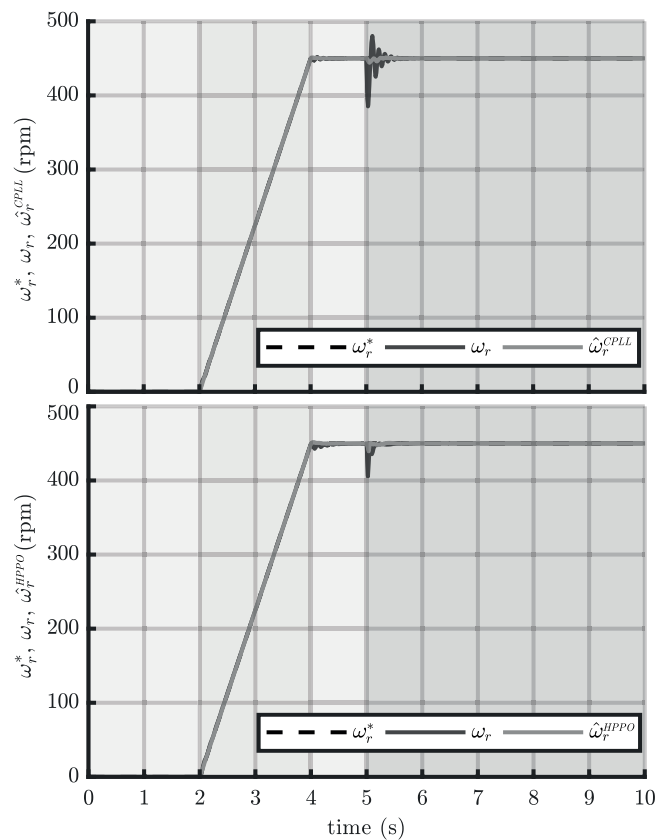


Fig. 4. Rotor speed control with IFOC using PLL observers: Conventional PLL (above) and High Performance PLL (below).

## VI. EXPERIMENTAL RESULTS

An experimental evaluation was carried out to verify the operation of the proposed PLL technique in practical operation conditions. Experimental results obtained during tests validate the IFOC control system, the CPLL, and the HPPO observers.

The drive prototype consists basically of a three-phase rectifier, a full bridge PWM inverter, a three induction motor, a measurement system, and a digital signal processor. An LC filter is used smooth the input currents and generate the inverter DC bus. As a load, a permanent magnet synchronous generator is used. This generator is connected to a resistor

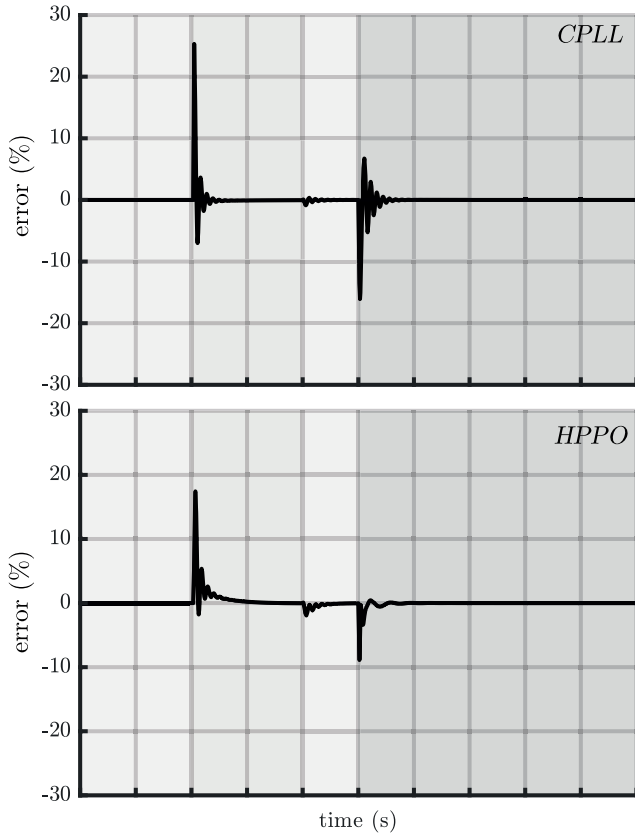


Fig. 5. Observer errors: CPLL (above) and HPPO (bellow).

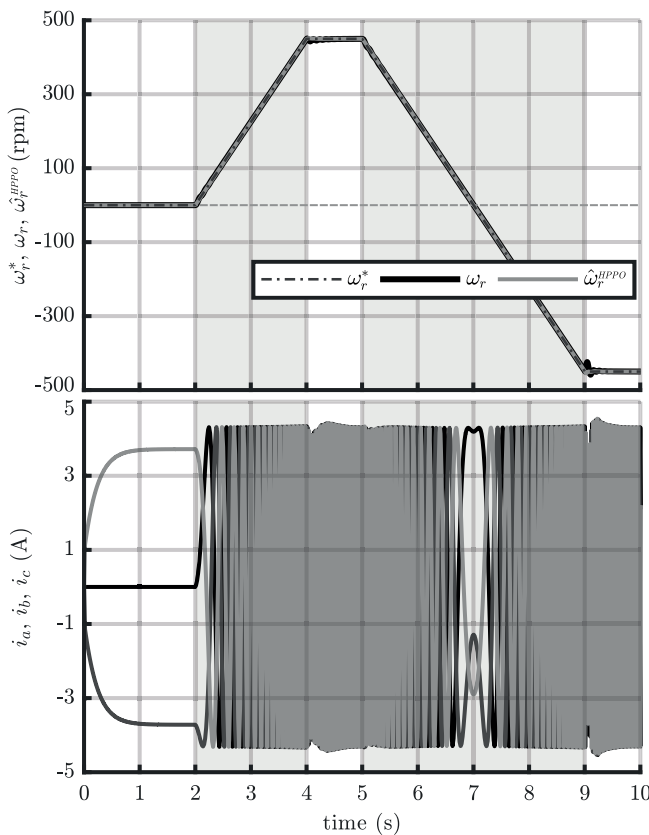


Fig. 6. IM drive performance during motor speed reversal: rotor speed (above) and stator currents (below).

module, operated using circuit breakers. Figure 7 shows the diagram of the drive prototype.

The currents measurement system consists of hall-effect sensors and signal conditioning modules to adjust the measured signals to levels appropriate to the DSP. Low-pass filtering is performed in these modules to eliminate noise from the inverter switching, thus improving system control. A digital signal processor (DSP-TMS320F28069M) is used to implement the control routines and generation of PWM signals that feed the inverter. The components used in the drive platform are in the Table II.

TABLE II  
Drive Prototype Components

Component	Model
Rectifier Module	SKKH 42/08E
Bus Capacitor	4700 $\mu F$ 450 V
Filter Inductor	2 mH
IGBT	SKM750GB063D
Driver	SKHI22AR
Encoder	AC-58
Processor	TMS320F28069M
Current Sensor	LA55-P
Operational Amplifiers	INA128/AD708
Buffer	SB7407

The experimental evaluation considered the same reference profiles used in the simulation analysis. A ramp from 0 to 450rpm during 2s is applied as speed reference in first tests to verify the performance of IFOC and PLL schemes to work together. In the sequence, the reference profile is changed to motor speed reversal (0  $\rightarrow$  450rpm  $\rightarrow$  -450rpm).

#### A. CPLL - Experimental Results

Figure 8 shows the actual and estimated speed for CPLL estimation scheme. It can be verified the insertion of dynamics in the real speed, besides the error in the starting of the machine. This error arises because the dynamics associated with the PLL observer are faster than the mechanical dynamics of the machine. A small estimation error is still present in steady-state operation.

#### B. HPPO - Experimental Results

The HPPO estimation result is shown in Figure 9. One can notice the behavior of the speed estimation very close to the actual speed. Moreover, the HPPO leads to lower insertion of dynamics in the rotor speed, besides the almost null error during the motor drive transient as well in steady-state operation.

Figure 10 shows the behavior of the HPPO estimator with motor speed reversal. The actual rotor speed follows the reference closely, and the speed estimation is used in the closed-loop control system. The motor operation is analogous to that of the Figure 6. The currents that feed the motor are very similar to the numerical analysis, both in motor starting and motor speed reversal.

The behavior of the system with the load removal was also evaluated, depicted in Figure 11. The IM machine is driven with a load of 3Nm on its shaft at the motor start. After the machine enters a steady-state, the load is removed. It

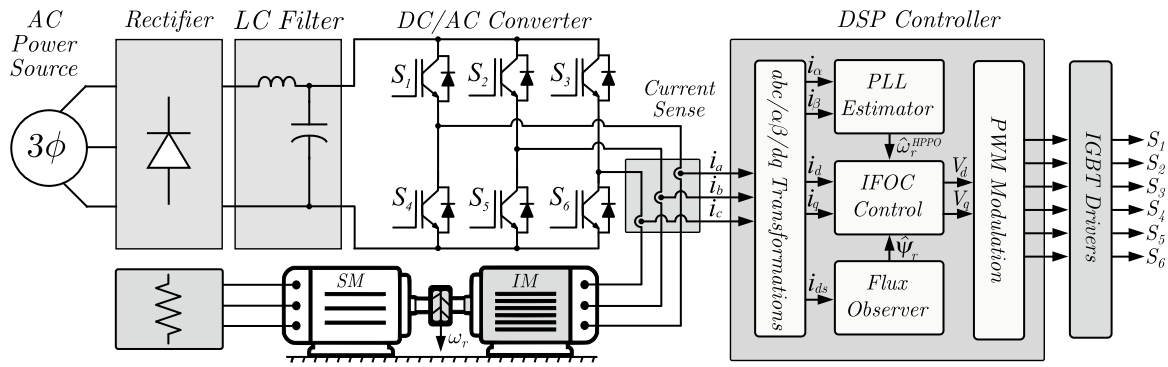


Fig. 7. Diagram of the laboratory prototype of induction motor drive.

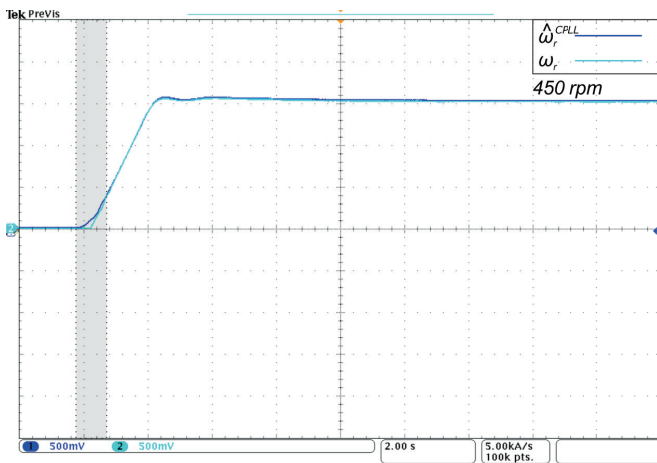


Fig. 8. Actual and estimated rotor speed using CPLL algorithm.

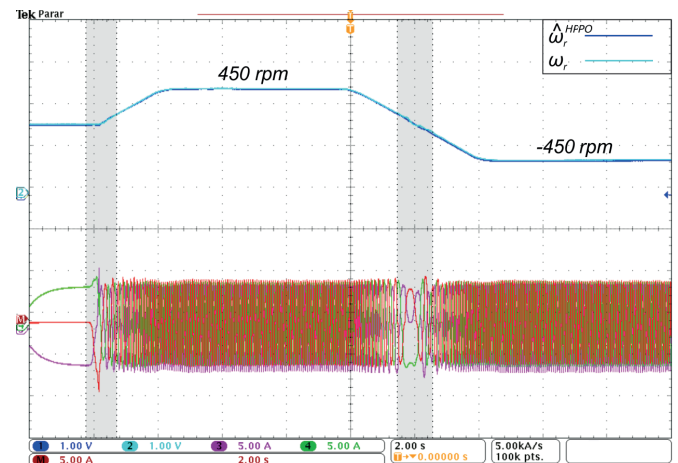


Fig. 10. HPPO estimation and actual speed for motor speed reversal.

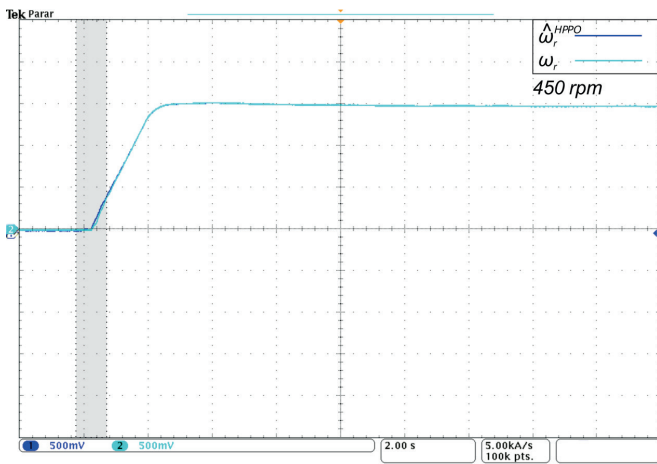


Fig. 9. Actual and estimated rotor speed using the HPPO algorithm.

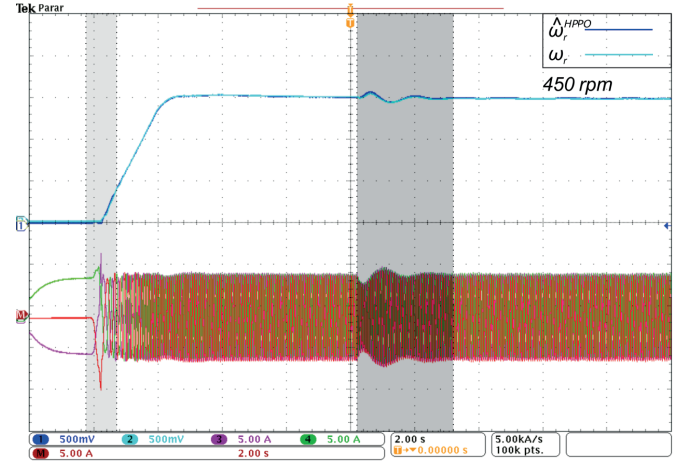


Fig. 11. HPPO estimation and stator currents for load removal.

is possible to verify the excellent performance of the speed control system and the correct operation of the HPPO, carrying on to estimate the speed during the whole operation of the motor drive.

## VII. CONCLUSIONS

This paper presented a modified PLL observer for improved rotor speed estimation in three-phase induction motors. The proposed observer is called High-Performance PLL Observer (HPPO). First, the mathematical modeling of the three-phase induction motor is presented in a generic reference,

along with the IFOC control system and the design of the controllers' gains. The mathematical model of the PLL observer in quadrature ( $\alpha\beta \rightarrow dq$ ) is raised. Then, the proposed modifications are included in the conventional PLL observer (CPLL) to derive the HPPO speed estimator.

- Numerical analyses were performed to verify the proposed HPPO performance and compare it with the CPLL. For both cases, speed and load variation are considered. The relative errors from estimated to the actual rotor speed were analyzed, and it was verified that the HPPO had significantly smaller errors in all cases.
- Using a laboratory prototype, experimental results were

obtained for both CPLL and HPPO estimators. The experimental analysis confirmed to numerical results since the motor drive prototype resulted in similar characteristics to the simulation one.

- The experimental evaluation shows that the HPPO algorithm results in significant better speed estimation than the CPLL. The main advantages verified are the lower estimation error at the motor start as well in steady-state, lower oscillations in transients, and good performance at full speed range, even during motor speed reversal.

#### ACKNOWLEDGEMENTS

The authors thank the Fundacao Araucaria, CAPES, Conselho Nacional de Desenvolvimento Cientifico e Tecnologico (CNPq), and Universidade Tecnologica Federal do Parana (UTFPR) for the support for this work.

#### REFERENCES

- [1] J. Holtz, J. Quan, J. Pontt, J. Rodriguez, P. Newman, H. Miranda, "Design of fast and robust current regulators for high-power drives based on complex state variables", *IEEE Transactions on Industry Applications*, vol. 40, no. 5, pp. 1388–1397, Sep. 2004, doi:10.1109/TIA.2004.834049.
- [2] H. T. Câmara, H. A. Grundling, "A MMRAC Controller Applied To Encoderless Speed Control Induction Motor Drives", *Revista Eletrônica de Potência*, vol. 10, no. 2, pp. 49–56, Nov. 2005, doi: 10.18618/REP.2005.2.049056.
- [3] F. Blaschke, "The principle of field orientation as applied to the new transvector closed loop system for rotating field machines", *Siemens Rev*, vol. 39, no. 5, pp. 217–220, May 1972.
- [4] J. Holtz, "Pulsewidth modulation for electronic power conversion", *Proceedings of the IEEE*, vol. 82, no. 8, pp. 1194–1214, Aug. 1994, doi:10.1109/5.301684.
- [5] Z. M. Elbarbary, H. A. Hamed, E. E. El-Kholy, "Comments on Performance Investigation of a Four-Switch Three-Phase Inverter-Fed IM Drives at Low Speeds Using Fuzzy Logic and PI Controllers", *IEEE Transactions on Power Electronics*, vol. 33, no. 9, pp. 8187–8188, Sept 2018, doi:10.1109/TPEL.2017.2743681.
- [6] I. M. Mehedi, N. Saad, M. A. Magzoub, U. M. Al-Saggaf, A. H. Milyani, "Simulation Analysis and Experimental Evaluation of Improved Field-Oriented Controlled Induction Motors Incorporating Intelligent Controllers", *IEEE Access*, pp. 1–1, Feb. 2022, doi: 10.1109/ACCESS.2022.3150360.
- [7] T. H. dos Santos, A. Goedel, S. A. O. da Silva, M. Suetake, "Controle Escalar do Motor de Indução Usando a Técnica Sensorless Neural", *Revista Eletrônica de Potência*, vol. 19, no. 1, pp. 24–35, Feb. 2014, doi:10.18618/REP.2014.1.024035.
- [8] X. Fu, S. Li, "A Novel Neural Network Vector Control Technique for Induction Motor Drive", *IEEE Transactions on Energy Conversion*, vol. 30, no. 4, pp. 1428–1437, Dec. 2015, doi: 10.1109/TEC.2015.2436914.
- [9] Z. Yan, C. Jin, V. Utkin, "Sensorless sliding-mode control of induction motors", *IEEE Transactions on Industrial Electronics*, vol. 47, no. 6, pp. 1286–1297, Dec. 2000, doi:10.1109/41.887957.
- [10] C. Lascu, I. Boldea, F. Blaabjerg, "Direct torque control of sensorless induction motor drives: a sliding-mode approach", *IEEE Transactions on Industry Applications*, vol. 40, no. 2, pp. 582–590, Mar.-Apr 2004, doi:10.1109/TIA.2004.824441.
- [11] Z. Zhang, H. Xu, L. Xu, L. Heilman, "Sensorless direct field-oriented control of three-phase induction motors based on "Sliding Mode" for washing-machine drive applications", *IEEE Transactions on Industry Applications*, vol. 42, no. 3, pp. 694–701, May-Jun. 2006, doi:10.1109/TIA.2006.872919.
- [12] S. M. Gadoue, D. Giaouris, J. W. Finch, "MRAS Sensorless Vector Control of an Induction Motor Using New Sliding-Mode and Fuzzy-Logic Adaptation Mechanisms", *IEEE Transactions on Energy Conversion*, vol. 25, no. 2, pp. 394–402, Jun. 2010, doi:10.1109/TEC.2009.2036445.
- [13] C. Lascu, F. Blaabjerg, "Super-twisting sliding mode direct torque control of induction machine drives", in *2014 IEEE Energy Conversion Congress and Exposition (ECCE)*, pp. 5116–5122, 2014, doi: 10.1109/ECCE.2014.6954103.
- [14] H. Wang, X. Ge, Y.-C. Liu, "Second-Order Sliding-Mode MRAS Observer-Based Sensorless Vector Control of Linear Induction Motor Drives for Medium-Low Speed Maglev Applications", *IEEE Transactions on Industrial Electronics*, vol. 65, no. 12, pp. 9938–9952, Dec. 2018, doi:10.1109/TIE.2018.2818664.
- [15] M. Zand, M. Azimi Nasab, M. Khoobani, A. Jahangiri, S. Hossein Hosseinian, A. Hossein Kimiai, "Robust Speed Control for Induction Motor Drives Using STSM Control", in *2021 12th Power Electronics, Drive Systems, and Technologies Conference (PEDSTC)*, pp. 1–6, 2021, doi: 10.1109/PEDSTC52094.2021.9405912.
- [16] S. K. Kakodia, G. Dynamina, "A Comparative Study of DFOC and IFOC for IM Drive", in *2020 First IEEE International Conference on Measurement, Instrumentation, Control and Automation (ICMICA)*, pp. 1–5, 2020, doi: 10.1109/ICMICA48462.2020.9242909.
- [17] P. Vas, *Sensorless vector and direct torque control*, Oxford University Press, 1998.
- [18] D. D. Pinheiro, C. M. O. Stein, J. P. Costa, R. Cardoso, E. G. Carati, "Comparison of sensorless techniques based on Model Reference Adaptive System for induction motor drives", in *2015 IEEE 13th Brazilian Power Electronics Conference and 1st Southern Power Electronics Conference (COBEP/SPEC)*, pp. 1–6, Nov. 2015, doi:10.1109/COBEP.2015.7420106.
- [19] J. Holtz, "Sensorless control of induction motor drives", vol. 90, no. 8, pp. 1359–1394, Aug. 2002.

- [20] J. Holtz, J. Quan, "Sensorless vector control of induction motors at very low speed using a nonlinear inverter model and parameter identification", *IEEE Transactions on Industry Applications*, vol. 38, no. 4, pp. 1087–1095, July 2002, doi: 10.1109/TIA.2002.800779.
- [21] C. Schauder, "Adaptive speed identification for vector control of induction motors without rotational transducers", *IEEE Transactions on Industry Applications*, vol. 28, no. 5, pp. 1054–1061, Sep. 1992, doi:10.1109/28.158829.
- [22] L. Ben-Brahim, S. Tadakuma, A. Akdag, "Speed control of induction motor without rotational transducers", *IEEE Transactions on Industry Applications*, vol. 35, no. 4, pp. 844–850, July 1999, doi:10.1109/28.777193.
- [23] C. Lascu, I. Boldea, F. Blaabjerg, "A modified direct torque control for induction motor sensorless drive", *IEEE Transactions on Industry Applications*, vol. 36, no. 1, pp. 122–130, Jan. 2000, doi:10.1109/28.821806.
- [24] H. Kubota, K. Matsuse, T. Nakano, "DSP-based speed adaptive flux observer of induction motor", *IEEE Transactions on Industry Applications*, vol. 29, no. 2, pp. 344–348, March 1993, doi:10.1109/28.216542.
- [25] S.-H. Kim, T.-S. Park, J.-Y. Yoo, G.-T. Park, "Speed-sensorless vector control of an induction motor using neural network speed estimation", *IEEE Transactions on Industrial Electronics*, vol. 48, no. 3, pp. 609–614, June 2001, doi:10.1109/41.925588.
- [26] V. I. Utkin, "Variable structure systems with sliding modes", *IEEE Transactions on Automatic Control*, vol. 22, no. 2, pp. 212–22, April 1977, doi: 10.1109/TAC.1977.1101446.
- [27] A. Sabanovic, D. B. Izosimov, "Application of Sliding Modes to Induction Motor Control", *IEEE Transactions on Industry Applications*, vol. IA-17, no. 1, pp. 41–49, Jan. 1981, doi: 10.1109/TIA.1981.4503896.
- [28] V. I. Utkin, J. Guldner, M. Shijun, "Sliding mode control in electromechanical systems", in *IEEE Decision and Control Conference*, pp. 4591–4596, 1996.
- [29] A. D. Gloria, D. Grosso, M. Olivieri, G. Restani, "A novel stability analysis of a PLL for timing recovery in hard disk drives", *IEEE Transactions on Circuits and Systems I: Fundamental Theory and Applications*, vol. 46, no. 8, pp. 1026–1031, Aug. 1999, doi: 10.1109/81.780384.
- [30] L. Harnefors, H. . Nee, "A general algorithm for speed and position estimation of AC motors", *IEEE Transactions on Industrial Electronics*, vol. 47, no. 1, pp. 77–83, Feb. 2000, doi:10.1109/41.824128.
- [31] M. Comanescu, L. Xu, "An improved flux observer based on PLL frequency estimator for sensorless vector control of induction motors", *IEEE Transactions on Industrial Electronics*, vol. 53, no. 1, pp. 50–56, Feb. 2006, doi:10.1109/TIE.2005.862317.
- [32] M. H. Bierhoff, "A General PLL-Type Algorithm for Speed Sensorless Control of Electrical Drives", *IEEE Transactions on Industrial Electronics*, vol. 64, no. 12, pp. 9253–9260, Dec. 2017, doi: 10.1109/TIE.2017.2711568.
- [33] D. D. Pinheiro, E. G. Carati, F. S. D. Sant, J. P. d. Costa, R. Cardoso, C. M. P. de Stein, "Improved Sliding Mode and PLL Speed Estimators for Sensorless Vector Control of Induction Motors", in *2018 13th IEEE International Conference on Industry Applications (INDUSCON)*, pp. 1030–1037, 2018, doi: 10.1109/INDUSCON.2018.8627293.
- [34] P. Mishra, C. Lascu, M. M. Bech, B. Rannestad, S. Munk-Neilsen, "Design and Analysis of PLL Speed Estimator for Sensorless Rotor-Flux Oriented Control of Induction Motor Drives", in *2021 IEEE Energy Conversion Congress and Exposition (ECCE)*, pp. 4743–4747, 2021, doi: 10.1109/ECCE47101.2021.9595316.
- [35] D. D. Pinheiro, *Analysis and proposition of strategies estimation and speed control for induction motors three-phase*, Federal University of Technology - Parana, 2016.
- [36] P. Krause, O. Wasynczuk, S. D. Sudhoff, S. Pekarek, *Analysis of electric machinery and drive systems*, vol. 75, John Wiley Sons, 2013.
- [37] R. Teodorescu, M. Liserre, P. Rodriguez, *Grid converters for photovoltaic and wind power systems*, vol. 29, John Wiley Sons, Ltd, Dec. 2010, doi: 10.1002/9780470667057.
- [38] G. F. Franklin, J. Powell, A. Emami-Naeini, *Feedback Control of Dynamic Systems*, ISBN 9780133496598, JPrentice Hall, Jan. 2002.

## BIOGRAPHIES

**Emerson Giovanni Carati**, born in 1974 in Palmitinho, Brazil. He received the B. S. degree (1996), the Master degree (1999) and PhD degree (2003) in Electrical Engineering from Federal University of Santa Maria (UFSM), Brazil. Since 2003, he is with the Federal University of Technology - Paraná (UTFPR), Pato Branco where he is Titular Professor. His research interests are related to control of electrical machines drives, distributed power generation and static converters.

**Felipe Sassi Del Sant**, born in 1996 in Sarandi, Brazil. He currently works as a data scientist and is a master's student in electrical engineering at the Federal University of Santa Catarina (UFSC). He holds a degree in electrical engineering from UTFPR, Pato Branco. He is interested in the areas of digital signal processing, machine learning and computer vision.

**Diego Dias Pinheiro**, born in 1991 in Foz do Iguacu, Brazil. He received the B.Sc and M.Sc. degrees from the Federal University of Technology - Paraná (UTFPR), Pato Branco, Brazil, 2014 and 2016, respectively all in Electrical Engineering. He is currently a Ph.D student in electrical and computer engineering from State University of Campinas (UNICAMP), Campinas, Brazil. His main interests are in the field of control of electrical drives, power electronics, renewable energy, predictive and sensorless control of electrical drives, and artificial neural networks.